EFDA–JET–PR(10)57

H. Urano, G. Saibene, N. Oyama, V. Parail, P. de Vries, R. Sartori, Y. Kamada,
K. Kamiya, A. Loarte, J. Lönnroth, Y. Sakamoto, A. Salmi, K. Shinohara,
H. Takenaga, M. Yoshida, The JT-60 Team
and JET EFDA contributors

Edge Pedestal Characteristics in JET and JT-60U Tokamaks Under Variable Toroidal Field Ripple

Edge Pedestal Characteristics in JET and JT-60U Tokamaks Under Variable Toroidal Field Ripple

H. Urano[1], G. Saibene[2], N. Oyama[1], V. Parail[3], P. de Vries[4], R. Sartori[2], Y. Kamada[1], K. Kamiya[1], A. Loarte[2], J. Lönnroth[5], Y. Sakamoto[1], A. Salmi[5], K. Shinohara[1], H. Takenaga[1], M. Yoshida[1], The JT-60 Team[6]
and JET EFDA contributors*

JET-EFDA, Culham Science Centre, OX14 3DB, Abingdon, UK

[1]Japan Atomic Energy Agency, Naka Fusion Institute, Naka, 311-0193, Japan
[2]Fusion for Energy, Torres Diagonal Litoral Edificio B3, 08019 Barcelona, Spain
[3]EFDA-JET, Culham Science Centre, OX14 3DB, Abingdon, OXON, UK
[4]FOM Rijnhuizen, Association EURATOM-FOM, Netherlands
[5]Association Euratom-Tekes, Helsinki University of Technology, Finland
[6]See the Appendix of A. Isayama et al., Proceeding of IAEA Fusion Energy Conbference 2010 Korea, Daejon
** See annex of F. Romanelli et al, "Overview of JET Results",*
(23rd IAEA Fusion Energy Conference, Daejon, Republic of Korea (2010)).

Preprint of Paper to be submitted for publication in
Nuclear Fusion

ABSTRACT.
The effect of Toroidal Field (TF) ripple on the edge pedestal characteristics were examined in the TF ripple scan experiments at the plasma current I_p of 1.1MA in JET and JT-60U. The TF ripple amplitude δR was defined as a value averaged over the existing ripple wells at the separatrix on the outer midplane. By the installation of Ferritic Inserts (FIs), δ_R was reduced from 1% to 0.6% at 3.2T (0.5% at 2.2T) in JT-60U. In JET, δ_R was varied from 0.08% to 1% by feeding different currents to the odd and even set of coils out of 32 TF coils. The pedestal pressure pped was similar for the cases before and after the installation of FIs in JT-60U. Similarly, no clear difference in pped was also observed in the variation of δ_R in JET. The core and edge toroidal rotation clearly decreased in counter direction by increased δ_R. However, there were no changes in the spatial profiles of electron density, electron temperature and ion temperature. By the installation of FIs in JT-60U, the ELM frequency f_{ELM} decreased by ~20%, while the ELM energy loss increased by 50–150%. The increased ELM loss power by 30% suggests a reduction of inter-ELM transport with the reduced δ_R. In JET, f_{ELM} increased only slightly with increased δ_R while the edge toroidal rotation frequency decreased as δ_R increased. From the inter-machine similarity experiment at 1.1MA, TF ripple less than 1% does not strongly affect the pedestal pressure. However, in the single TF ripple scan at the higher I_p of 2.6MA in JET, it clearly decreases with the increased δ_R, accompanying with a strong density pump out at large TF ripple. These results suggets that the effect of TF ripple on H-mode properties becomes stronger in the plasmas with higher I_p or lower edge collisionality.

1. INTRODUCTION

The H-mode operation with high fusion gain ($Q_{DT} > 10$) is required in ITER with a large fraction of the plasma heating supplied by the α-particles from fusion reactions. For the goal of ITER, this requires both thermal and fast ion confinement to be at sufficiently high performance. In H-mode plasmas, the edge pedestal structure characterized by the formation of the Edge Transport Barrier (ETB) is known to determine the boundary condition of the heat transport in the plasma core as well as the characteristics of the Edge-Localized-Modes (ELMs). It is one of the crucial concerns that the Toroidal magnetic Field (TF) ripple structure may affect the H-mode confinement in ITER. In tokamaks, the finite number and toroidal extension of the TF coils causes a periodic variation of the toroidal magnetic field from its nominal value, which is called TF ripple δ_R. The TF ripple in the toroidal magnetic field adversely affects fast ion confinement by modifying the guiding center orbits of fast ions. ITER is equipped with 18 TF coils, and the basic level of TF ripple is relatively high, ~1.2% at the nominal separatrix position in the outer midplane. The TF ripple could primarily induce the reduction of the heating efficiencies due to the enhanced TF ripple induced losses of ripplebanana diffusion and ripple-trapped transport. In addition, the existence of large TF ripple could also induce excessive heat loads to limiters and other plasma-facing components. For avoiding these risks during discharges particularly at high performance, the installation of ferromagnetic materials is expected to reduce the TF ripple. In ITER, the Ferritic Inserts (FIs) compensation is

included in the design, reducing δR from ~1.2% to ~0.35%. It was investigated that the ferromagnetic components were effective on energetic ion confinement in the present ITER operation scenarios [1]. The influence of the TF ripple on the fast ion losses were examined in JT-60U by the installation of FIs [2]. Besides, the dedicated TF ripple scan experiments were also conducted in JET [3]. While the TF ripple affects primarily the fast ion losses, both experiments have indicated that ripple may also affect the H-mode confinement and plasma rotation [4]. It is presumed that in the peripheral region an inward electric field produced by the TF ripple induced losses drives the toroidal rotation V_T in the counter direction to the plasma current I_p [5,6]. However, the underlying physics for the reduction of the energy confinement with δ_R was not clearly understood.

Inter-machine experiments between JET and JT-60U have been performed to compare H-mode pedestal performance and ELM characteristics using matched plasma shape at 1.1MA. Inter-machine experiment is a very powerful tool to identify the physics mechanisms determining the plasma behavior, as well as a way to validate the assumptions behind the physics based scaling used for the prediction of the plasma parameters of ITER. In the previous experiments, MHD stability analysis shows that the pedestal MHD stability of both tokamaks is similar and probably cannot explain the observed difference in ELMy H-mode performance [7]. The TF ripple structure and consequently different toroidal rotation profiles have been pointed out as major remaining differences between two devices, as shown in figure 1. Therefore, new similarity experiments focused on TF ripple and toroidal rotation profile have been performed in both devices [8]. In addition, a single TF ripple scan experiments were also carried out in JET at higher I_p of 2.6MA using the JET standard configuration. The ITER will operate at much lower edge collisionality of $\nu^*_{ped} < 0.01$ than present devices. The influence of TF ripple on edge pedestal characteristics at higher I_p leading to lower ν^*_{ped} is also an important issue to be examined for ITER.

This paper reports the results of these experiments. The paper is organized as follows. After the introduction, the definition of TF ripple amplitude is proposed in section 2. The experimental conditions of the similarity experiment and the response of the plasma toroidal rotation at the pedestal are described in section 3. The influences of TF ripple and edge toroidal rotation on the H-mode performance and pedestal are described in section 4. The ELM characteristics are also compared in this section. In addition to the similarity experiment at lower I_p, the effect of TF ripple on pedestal characteristics at higher I_p conducted in JET TF ripple scan experiment is described in section 5. Finally, a summary is given in section 6.

2. DEFINITION OF TF RIPPLE AMPLITUDE

The TF ripple is a fluctuating structure of the TF strength induced by the finite number of the TF coils. Therefore, different number and shape of TF coils causes essentially different TF ripple amplitude and topology as shown in figure 1. JT-60U has 18 circular TF coils and thus the contour plot of TF ripple amplitude shows a circular shape, while 32 D-shape coils are equipped in JET resulting in relatively small TF ripple with Dshaped contours. In this paper, the local TF ripple value at the

separatrix on the outer midplane is taken as the representative TF ripple amplitude. Figure 2(a) shows the BT along the toroidal angle at the separatrix on the outer midplane in JT-60U. By the installation of FIs, the fluctuation of B_T along the toroidal angle is moderated. Due to the existence of tangential NB ports where FIs cannot be installed, the magnetic structure became more complex. Figure 2(b) plots the TF ripple value calculated by $\delta_R = (B_{TMax} - B_{TMin})/(B_{TMax} + B_{TMin})$ at each ripple well (every 20 degree). While δ_R is uniform at ~1% before the FI installation, δ_R is scattered at reduced values at all sections after the FI installation. Figure 3 shows the TF ripple averaged over all sections between 2 TF coils evaluated along the separatrix in the plasma configuration for the similarity experiment for the cases of JT-60U and JET. The magnetic axis corresponds to Z = 0.2m in JT-60U and Z = 0m in JET. In JT-60U, δ_R is gradually increased with increasing Z value and reaches the maximum at Z = 0.9m. One can find that δ_R was largely reduced around the outer midplane from 1% to 0.6% at Z = 0.2m while δ_R at the location where the TF ripple becomes the maximum was reduced from 1.3% to 0.7% (Z = 0.9m). On the other hand, δ_R has the peak at Z = 0.2m and gradually decreases with increasing Z value in JET. In this paper, considering the situation where the identical plasma configuration is used in the similarity experiment, TF ripple amplitude is defined as a value at the separatrix on the outer midplane.

3. EXPERIMENTS ON VARIABLE TF RIPPLE

The TF ripple scan experiments were conducted using essentially different methods in JET and JT-60U. In JET, the TF system can be configured to feed different currents to the odd and even set of coils out of 32 TF coils. In this operation mode, δ_R can actively be varied by selecting the appropriate differential current between each set of coils. In this experiment, four levels of δ_R = 0.08%, 0.5%, 0.75% and 1% were used. On the other hand, in JT-60U, the Ferritic Inserts (FIs) were installed in the vacuum vessel to reduce the TF ripple with enhancing the V_T in co-direction in 2005 [2]. It was reported in JT-60U that ELMy H-mode plasmas with VT in co-direction tend to have higher energy confinement than those in counter-direction [4]. In the present study, comparing between the plasmas with and without FIs, the effects of the TF ripple on the pedestal and core confinement properties can be examined. The FIs are optimized for TF ripple reduction at $B_T < 2T$ [2]. Since the magnetic field produced by FIs is saturated at 1.78T for $B_T \geq 0.6T$, δ_R can be varied with BT in JT-60U even after the installation of FIs. The similarity experiments with variable TF ripple were carried out at the lower values of I_p = 1.1MA and B_T = 2.0T. This is because this condition is the experiment point where the TF ripple magnitude could be better matched, as well as based on the characteristics of the FI correction in JT-60U, which is not very effective at high B_T. Note that since the geometry of NB heating system is also totally different between both devices the spatial profiles of NB injected torque and fast ions losses are not the same.

Figure 4 shows the variation of the toroidal rotation frequency at the top of the H-mode pedestal V_T^{ped} as a function of δ_R. In the similarity experiment, the total torque injected by NBI was 5.5 – 8.5Nm in JET except for plasmas with low heating power ($P_{NBI} < 4MW$), and in JT-60U, ~5.5Nm

without FIs and 6 – 7.5Nm with FIs. In contrast to JET in which the injected torque is proportional to the heating power, the variation of torque in JT-60U is small because the number of tangential NBs is limited and the heating power is mainly varied by using perpendicular-NBs, which provide input torque only slightly. As a result, the toroidal rotation in JT-60U plasmas shifts relatively to counter due to the loss power of the fast ions from the perpendicular-NBIs. Since fast ion losses were reduced after the installation of FIs, V_T^{ped} shifted towards co-direction. On the other hand, according to the previous study described in Ref. [8], the fast ions loss fraction does not vary much over the δ_R scan in JET. Therefore, the toroidal rotation frequency in JET plasmas mainly related to the δ_R. For a similar level of torque input in both devices, the upper boundary of the achieved rotation frequency decreased with increasing δ_R.

The fast ion losses were evaluated using the Orbit-Following Monte Carlo Code (OFMC) [9] in which the behavior of test particles for fast ions is traced until they are lost from the plasma or entirely thermalized. The OFMC code considers the ripple loss, the orbit loss and the charge exchange loss of the fast ions generated by NBI and estimates the density profile and the pressure profile of the fast ions, the profile of the NBI particle source and the energy deposition profiles to electrons and thermal ions.

4. EDGE PEDESTAL CHARACTERISTICS AND ELM BEHAVIOR

In this series of experiments, radial profiles of electron density ne and electron temperature T_e were measured with a Thomson scattering system, while ion temperature T_i was measured with Charge-eXchange Recombination Spectroscopy (CXRS) of carbon in JT-60U. On the other hand, n_e, T_e and T_i at the pedestal were measured with an edge chord of an FIR interferometer, Electron Cyclotron Emission (ECE) radiometer and CXRS in JET, respectively.

Figure 5(a) compares n_e^{ped} and T_e^{ped} in the TF ripple scan experiments in JT-60U. The achievable electron pressure at the pedestal p_e^{ped} was similar for the cases before and after the installation of FIs. For the case of δ_R ~0.5%, a moderate gas puffing to increase the plasma density made p_e^{ped} lower by ~20%. This result is identical to the dedicated H-mode experiments for a single TF ripple scan using two different plasma configurations in JT-60U [4]. Then, the pedestal pressure was clearly increased when δ_R was reduced from ~2% to ~1% using a large volume configuration (the separatrix of the configuration was close to the wall and $V_P \sim 75m^3$). No significant effect of TF ripple between plasmas with δ_R ~0.4% and δ_R ~0.2% was found with the small volume configuration (inward shifted plasma configuration with $V_P \sim 52m^3$), while the effect of TF ripple on toroidal rotation clearly observed in both plasma configurations.

In JET, newly analyzed data have been added from the previous result. Similarly to JT-60U, no clear difference of the pedestal n–T diagram was observed in the variation of the TF ripple as shown in figure 5(b). Figure 6 plots the dependence of pedestal pressure on δ_R with $P_{net} = 5.0 – 6.5MW$ in JET and $P_{net} = 6.0 – 8.0MW$ in JT-60U. In this similarity experiment, the change of the pedestal pressure is very weak and negligible to be quantified.

Figure 7 shows the spatial profiles of V_T, n_e, T_e and T_i in JET for the comparison of the TF ripple between 0.08% (P_{net}=6.1MW) and 1.0% (P_{net}=5.9MW). The edge toroidal rotation clearly decreases in counter direction by increased TF ripple. The core toroidal rotation profile also shifts towards the direction in counter. However, as expected from figure 5(b), there are no changes in n_e, T_e and T_i at the top of the Hmode pedestal. Besides, the changes of the core profiles of n_e, T_e and T_i are also very small. The similar result is obtained in a single TF ripple scan experiment conducted in JET [3], where the global and pedestal parameters of the 1MA/1T series of H-modes did not change significantly for increasing TF ripple. However, the effect of TF ripple on the edge toroidal rotation was still observed, and the edge toroidal rotation was reduced as the TF ripple was increased.

Figure 8 shows the dependence of ELM frequency fELM, ELM energy loss ΔW_{ELM}, pedestal toroidal rotation frequency V_T^{ped}, line-averaged electron density $\bar{n}e$, and total stored energy WDIA on the TF ripple amplitude in JT-60U. By the installation of FIs, the ELM frequency fELM decreased by ~30%, while the ELM energy loss ΔW_{ELM} increased by the factor of 2. The ELM loss power $f_{ELM} \cdot \Delta W_{ELM}$ increased by 30% for a given loss power through the separatrix P_{sep}. This result implies a reduction of inter-ELM transport with the reduced TF ripple. Because of the perpendicular-NB heating at large TF ripple, the edge toroidal rotation was in counter before the installation of FIs. By the reduction of TF ripple, the edge toroidal rotation frequency was explicitly varied towards the co-direction. While the inter-ELM transport is reduced by the reduction of TF ripple, the line-average electron density and total stored energy do not vary with TF ripple, similarly to almost no change in the pedestal pressure (see figure 6).

Figure 9(a) shows time evolution of the divertor Dα signal for the variation of TF ripple in JET. Since the type-I ELM frequency is increased in proportion to the power crossing the separatrix P_{sep}, P_{sep} is fixed at ~5MW. As shown in figure 9(b), ELM frequency increases only slightly with increasing TF ripple. The decrease of ELM energy loss is also small (see figure 9(c)). The edge toroidal rotation frequency decreases as the TF ripple increases (see figure 9(d)). Similarly to JT-60U, the line-averaged electron density and total stored energy do not vary with TF ripple (see figure 9(e)). From JT-60U result, the influence of TF ripple on the pedestal structure is small, but the ELM activity is more sensitively changed by TF ripple. In fact, this result has already been observed in the dedicated H-mode experiment for the cases before and after the installation of FIs in JT-60U [4]. However, in JET, the change of ELM activity in the variation of TF ripple is also small. According to the analysis done in the previous study [8], normalized ELM frequency is plotted as a function of the TF ripple and the pedestal toroidal rotation frequency in figure 10. As expected from figure 9(b), the change in ELM frequency in JET is smaller than that in JT-60U. Then, the variation of ELM frequency is examined as a function of the pedestal toroidal rotation frequency (see figures 10(c) and (d)). In both devices, the normalized ELM frequency decreases monotonically with increasing V_T^{ped} towards co-direction.

In this series of experiments, since the V_T^{ped} is simply changed by the variation of TF ripple, δ_R and V_T^{ped} vary monotonically together and thus it is hard to separate this relation. In the dedicated

H-mode experiment before and after the installation of FIs in JT-60U, the toroidal rotation scan was conducted by changing the direction of tangential NBs. In this case, ELM frequency clearly increased with enhanced pedestal toroidal rotation in counter at a given TF ripple [4]. On the other hand, in the single TF ripple scan experiment on JET, ELM frequency was essentially constant over the change of V_T^{ped} at 1MA and 1.7MA [3]. As a big difference between JET and JT-60U, the edge toroidal rotation in JET does not become negative while in the similar condition it does in JT-60U. However, in JET TF ripple scan experiment at 2.6MA, ELM frequency increased very clearly with increased TF ripple as described in section 5. In this experiment, V_T^{ped} became negative at 1% ripple. Nonetheless, ELM frequency changed largely in the range of positive V_T^{ped}. The other possibility is that the range of V_T^{ped} in JET might be too narrow to change the ELM activity compared to JT-60U. The change of V_T^{ped} is more significant at 2.6MA in a single TF ripple scan experiment on JET. In this experiment, ELM frequency increased very clearly with increased TF ripple. Further investigation is needed for the effect of toroidal rotation on ELMs.

5. THE EFFECT OF TF RIPPLE ON PEDESTAL CHARACTERISTICS AT HIGHER IP IN JET

As described in section 4, pped does not show clear change in the variation of TF ripple in both devices in the similarity experiment performed at 1.1MA. This result is basically consistent with the dedicated TF ripple scan experiment at 1MA in JET using the standard configuration, in which the global and pedestal parameters do not change for increasing TF ripple [3]. On the other hand, TF ripple scan experiments were also carried out at 2.6MA. Figure 11(a) shows the dependence of pedestal pressure p_{ped} on TF ripple δ_R for the JET and JT-60 similarity experiment at 1.1MA and the TF ripple scan at 2.6MA in JET. While p_{ped} do not change over the wide range of δ_R at 1.1MA, it clearly decreases with the increased δ_R at 2.6MA. The pedestal n – T diagram for JET 2.6MA TF ripple scan experiment is shown in figure 11(b). One can find that ranges of the pedestal electron density npede tend to shift towards lower values when TF ripple amplitude is raised. On the other hand, the pedestal electron temperature T_e^{ped} remains almost constant or slightly increased. This experimental result suggests that density pump out is enhanced with increased TF ripple particularly at higher I_p. While all observations above originate from plasmas with no gas fuelling in the H-mode phase, the effect of fuelling is investigated by adding increasing amounts of gas to the reference plasmas in JET [3]. It is reported that as the external gas fuelling is increased the difference of the steady state density achieved in the discharges between the cases of the minimum and maximum TF ripple becomes smaller.

In case of JET 2.6MA TF ripple scan, increasing δ_R at constant power across the separatrix (P_{sep} ~ 11MW) makes the type I ELM frequency f_{ELM} higher as plotted in figure 12(a). As δ_R is increased from 0.1% to 1.4%, f_{ELM} almost doubles, going from ~10Hz to ~28Hz, while ELM energy loss ΔW_{ELM} becomes monotonically smaller from ~500kJ to ~100kJ (see figure 12(b)). Therefore, the ELM loss power $f_{ELM} \cdot \Delta W_{ELM}$ gradually decreases with δR. This result implies the enhanced inter-

ELM transport with the increased TF ripple. As shown in figure 12(c), V_T^{ped} is drastically reduced with TF ripple and eventually becomes negative at 1.4% TF ripple. Similarly to the behavior of ripple scan experiment. pped, the stored energy W_{MHD} decreases with TF ripple (see figure 12(d)). In addition, density is drastically reduced when TF ripple is changed from 0.1% to 0.7%.

One of edge dimensionless parameters which differ largely between JET/JT-60U similarity experiment and JET 2.6MA TF ripple scan experiment is collisionality ν^*_{ped}(ρ^*_{ped} = 0.02–0.05, β_{p-ped} = 0.15–0.35). At $\bar{n}_e/n_{GW}$ = 0.4–0.5, the edge collisionality ν^*_{ped} ranges 0.05–0.5 in the similarity experiments while ν^*_{ped} ranges 0.01–0.02 in JET 2.6MA TF ripple scan experiment. One can find that the effect of TF ripple on H-mode properties (stored energy and density) varies depending on plasma background parameters. Focusing on the large difference of edge collisionalities between these experiments, the effect of TF ripple is clearly seen in plasmas accompanied with low edge collisionality in JET 2.6MA TF ripple scan while no significant difference is seen in the similarity experiment at 1.1MA. The ITER will operate at further low edge collisionality of $\nu^*_{ped} < 0.01$ with much higher Ip. There is no simple correlation between fast ion losses, torque, toroidal rotation and confinement explaining these experimental results. Thus, the ranges of other dimensionless parameters where the TF ripple affects strongly on the performance should be investigated particularly for the condition close to ITER as a next step study. In addition, the development of new models which can reproduce the response of plasmas to TF ripple is also urgently required for ITER.

SUMMARY

In this study, conducting the TF ripple scan experiments at 1.1MA in JET and JT-60U, the effect of TF ripple on the edge pedestal characteristics are examined. The TF ripple amplitude is defined as a value averaged over the existing ripple wells at the separatrix on the outer midplane. By the installation of FIs, TF ripple was reduced from 1% to 0.6% at 3.2T (0.5% at 2.2T) in JT-60U. In JET, the TF system can be configured to feed different currents to the odd and even set of coils out of 32 TF coils. In this operation mode, δ_R was actively varied by selecting the appropriate differential current between each set of coils. In this experiment, four levels of δ_R, 0.1%, 0.5%, 0.75% and 1%, were used. In addition, a single TF ripple scan experiments were also carried out in JET at higher I_p of 2.6MA using the JET standard configuration to investigate the influence of TF ripple on edge pedestal characteristics at low collisionality obtained at higher I_p.

In the similarity experiment at 1.1MA, the achievable electron pressure at the pedestal was similar for the cases before and after the installation of FIs in JT-60U. In JET, no clear difference of the pedestal n–T diagram was also observed in the variation of the TF ripple. The edge toroidal rotation clearly decreases in counter direction by increased TF ripple. The core toroidal rotation profile also shifts towards the direction in counter. However, there are no changes in n_e, T_e and T_i at the top of the H-mode pedestal. Besides, the changes of the core profiles of n_e, T_e and T_i are also very small. Dependence of ELM activity on the TF ripple amplitude was investigated. In JT-60U,

by the installation of FIs, the ELM frequency f_{ELM} decreased by ~30%, while the ELM energy loss ΔW_{ELM} increased by the factor of 2. The ELM loss power increased by ~30% for a given loss power through the separatrix P_{sep}, suggesting a reduction of inter-ELM transport with the reduced TF ripple. In JET, ELM frequency increases only slightly with increased TF ripple while the edge toroidal rotation frequency decreases as the TF ripple increased. The effect of TF ripple on ELM activity separated from the influence of pedestal toroidal rotation will be investigated as a next step study. A single TF ripple scan was also conducted at higher I_p of 2.6MA in JET. In this case, V_T^{ped} was drastically reduced with TF ripple and eventually became negative at 1.4% TF ripple. Besides, pedestal pressure clearly decreased with the increased δ_R accompanying with a strong density pump out. The ELM frequency also became higher with δ_R, and the inter-ELM transport was enhanced with the increased TF ripple. It seems that the effect of TF ripple on H-mode properties (stored energy and density) varies depending on plasma background parameters. One of edge dimensionless parameters which differ largely between JET/JT-60U similarity experiment and JET 2.6MA TF ripple scan experiment is collisionality. The ITER will operate at further low edge collisionality of $\nu^*_{ped} < 0.01$ with much higher I_p, where δ_R ranges 0.35– 1.2% when the FI compensation is included. There is no simple correlation between fast ion losses, torque, toroidal rotation and confinement explaining these experimental results. Thus, the investigation of the ranges of other dimensionless parameters where the TF ripple affects strongly on the performance is required particularly for the condition close to ITER as well as the development of new models which can reproduce the response of plasmas to TF ripple.

ACKNOWLEDGMENTS

They are also grateful to Drs M. Mori, T. Ozeki and T. Fujita of Japan Atomic Energy Agency for their encouragement and helpful advice. The diligent support of the JT-60 team is also cordially acknowledged.

REFERENCES

[1]. Shinohara K. et al., Fusion Engineering and Design **84** (2009) 24
[2]. Shinohara K. et al., in Proc. 21st IAEA Fusion Energy Conf., FT/P5-32 (Chendu, 2006)
[3]. Saibene G. et al., in Proc. 22nd IAEA Fusion Energy Conf., EX/2-1 (Geneva, 2008)
[4]. Urano H. et al., Nuclear Fusion **47** (2007) 706
[5]. Koide Y. et al., in Proc. 14th Int. Conf. W¨urzburg, 1992, IAEA, Vienna vol. 1 (1993) 777
[6]. Honda M. et al., Nuclear Fusion **48** (2008) 085003
[7]. Saibene G. et al., Nuclear Fusion **47** (2007) 969
[8]. Oyama N. et al., J. Phys.: Conf. Ser., 123 (2008) 012015
[9]. Shinohara K et al., Nuclear Fusion **43** (2003) 586

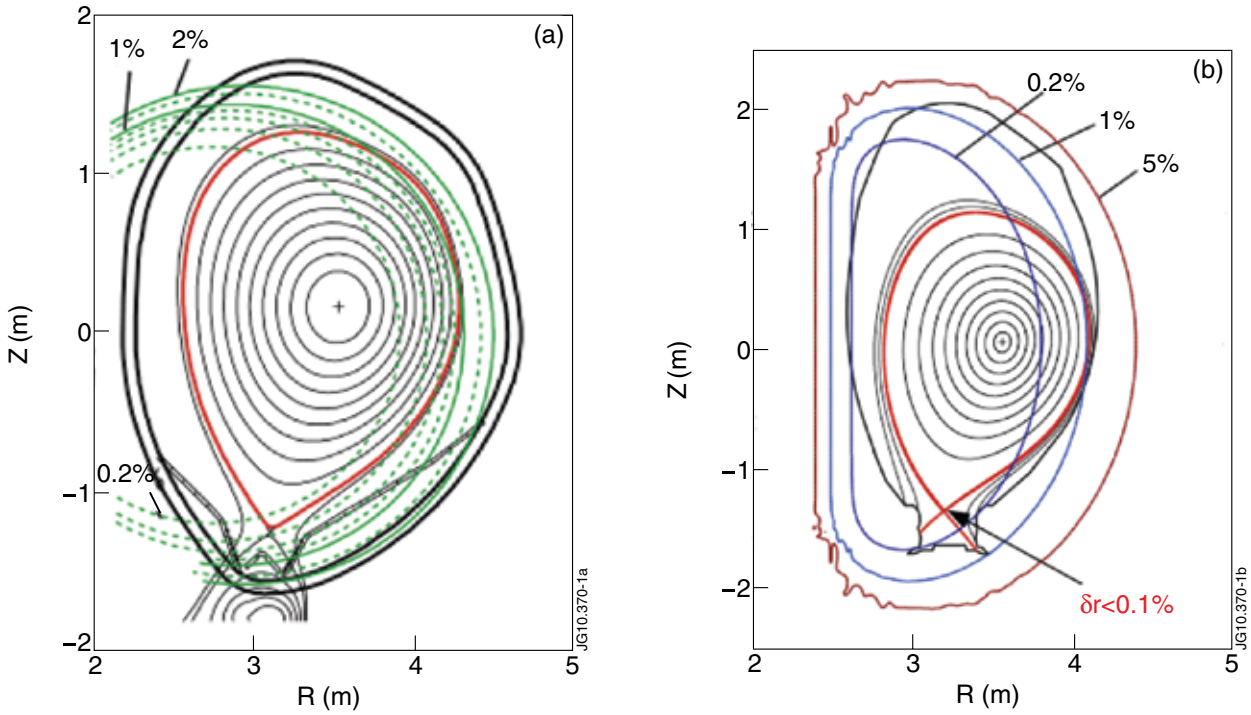

Figure 1:Plasma cross sections for the similarity experiments together with TF ripple contours in (a) JT-60U and (b) JET. Here, TF ripple amplitude is indicated by $(B_{TMax} - B_{TMin})/(B_{TMax} + B_{TMin})$. *The number of TF coils is 18 in JT-60U and 32 in JET.*

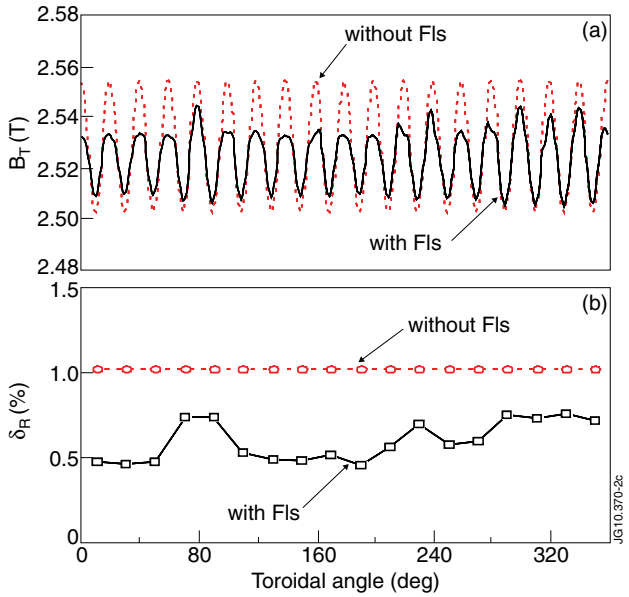

Figure 2: (a) The B_T *along the toroidal angle at the separatrix on the outer midplane (R = 4.28m, Z = 0.2m) for the cases before and after the installation of FIs in JT-60U. (b) The TF ripple at each section between 2 TF coils.*

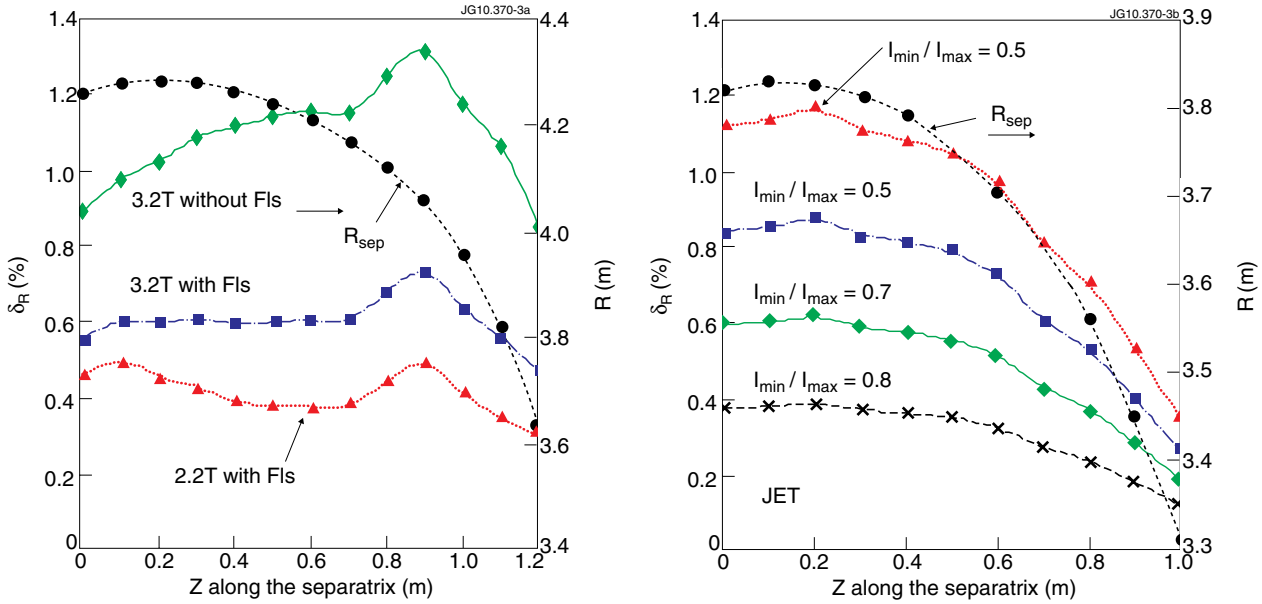

Figure 3: The local TF ripple value as a function of Z value along the separatrix in the configuration for the similarity experiment using (a) JT-60U and (b) JET TF coil system. I_{min}/I_{max} denotes the ratio of odd to even number of TF coils in JET. The major radius at the sepratrix Rsep gradually becomes smaller with increasing Z value.

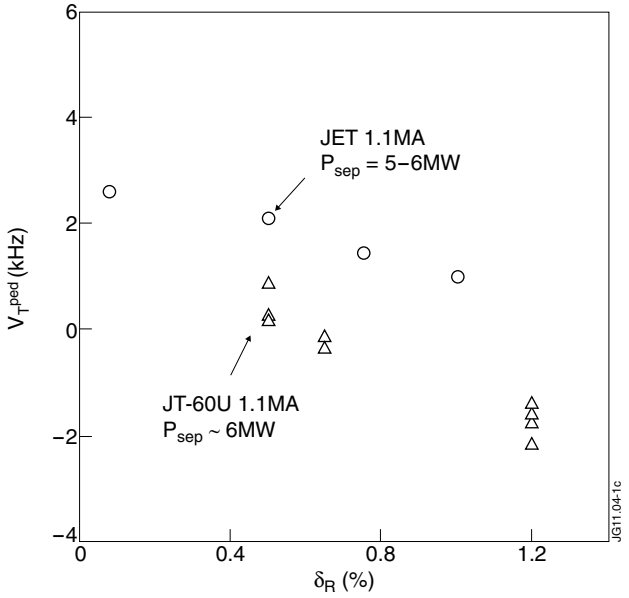

Figure 4: The toroidal rotation frequency at the H-mode pedestal shoulder V_T^{ped} as a function of δ_R. Circles and triangles indicate the data taken from the similarity experiment at 1.1MA in JET and JT-60U, respectively.

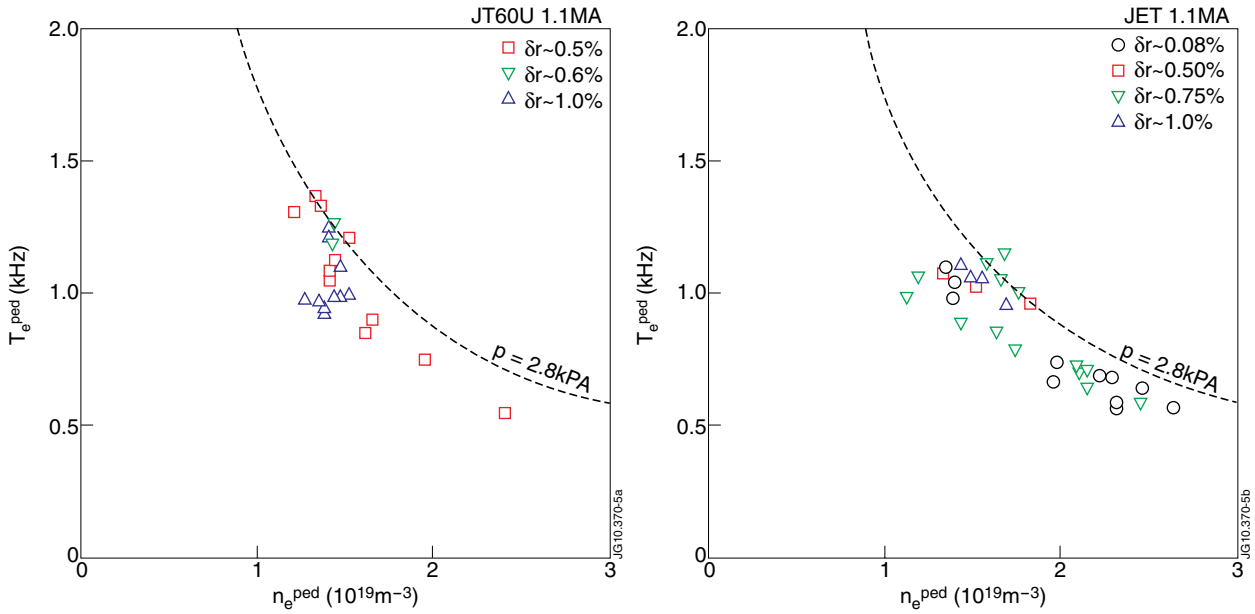

Figure 5: (a) The pedestal n−T diagram for the cases before and after the installation of FSTs in JT-60U at 1.1MA. (b) The pedestal n − T diagram in JET TF ripple scan experiment at 1.1MA. Broken curves indicate a constant electron pressure of 2.8kPa.

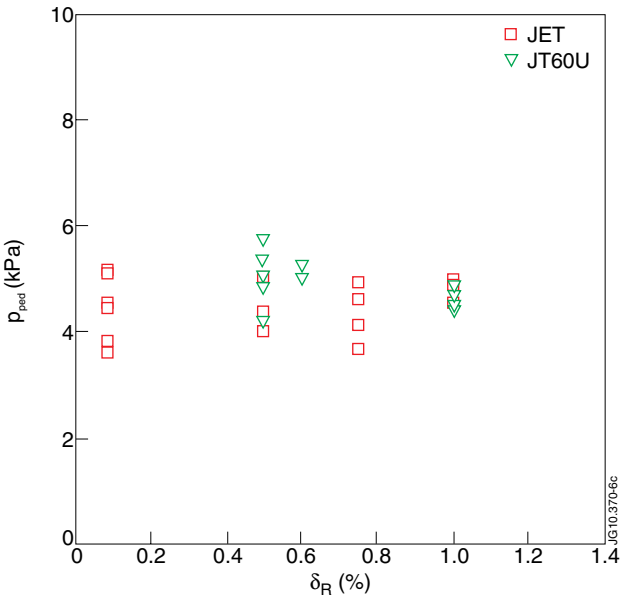

Figure 6: Dependence of pedestal pressure pped on TF ripple δ_R. Squares and inverse triangles denote the similarity experiment at 1.1MA in JET and JT-60U, respectively.

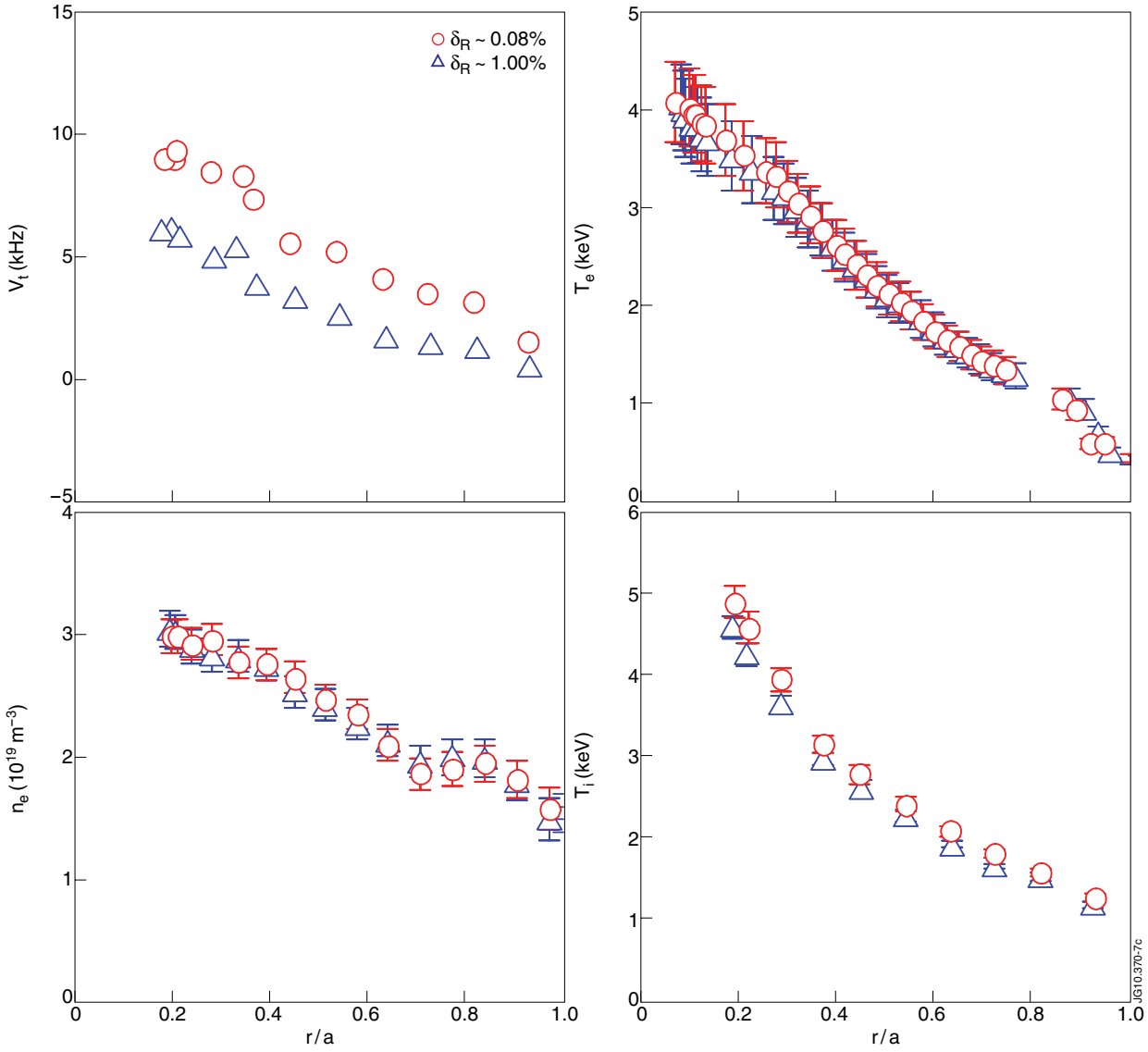

Figure 7: Spatial profiles of V_T, n_e, T_e and T_i for the TF ripple scan experiment in JET. Circles and triangles denote the TF ripple amplitude of 0.08% and 1.0%, respectively.

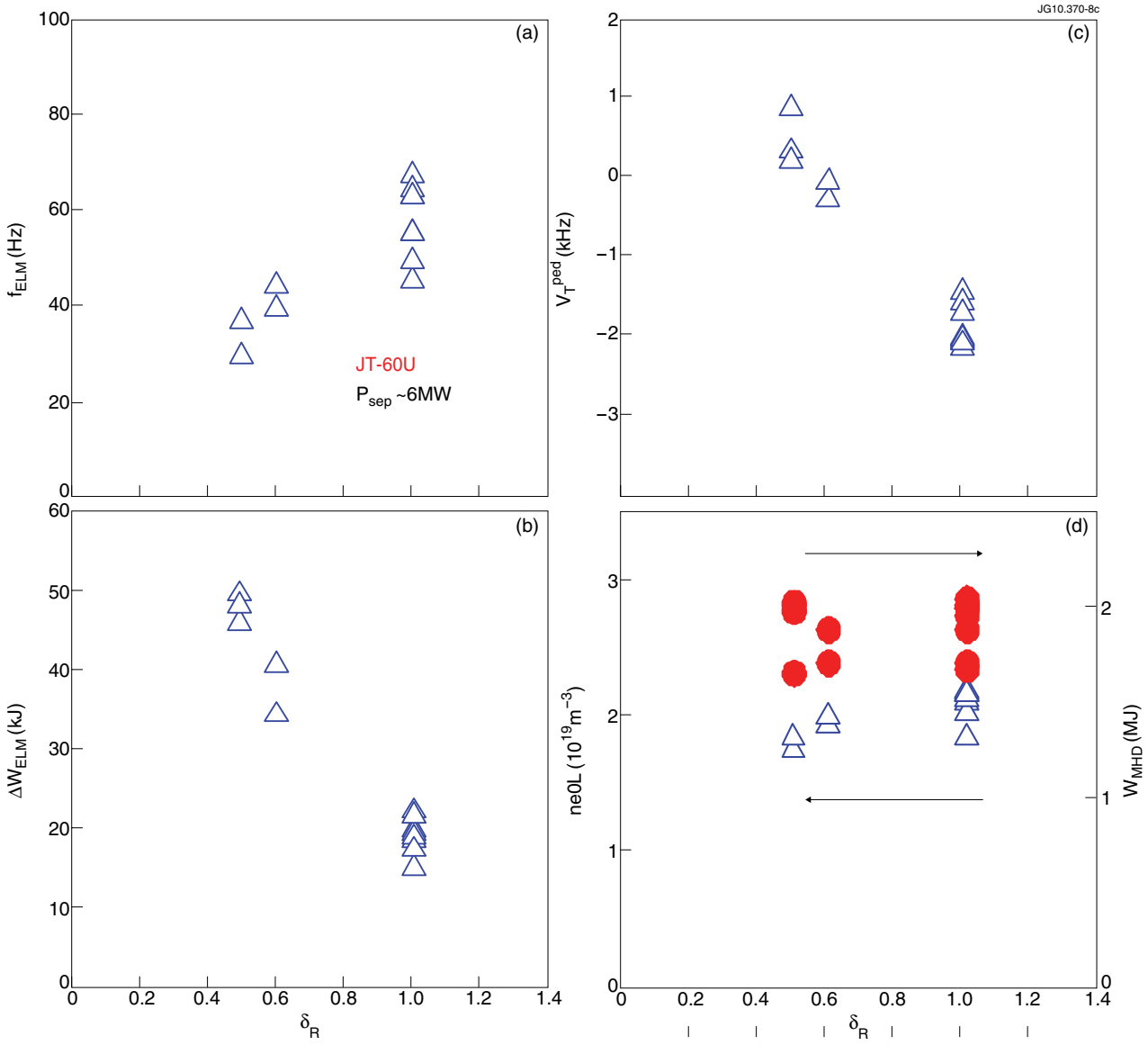

Figure 8: Dependence of (a) ELM frequency f_{ELM}, (b) ELM energy loss ΔW_{ELM}, (c) pedestal toroidal rotation frequency V ped T , (d) line-averaged electron density ¯ne, and total stored energy WDIA on the TF ripple amplitude δR in JT-60U.

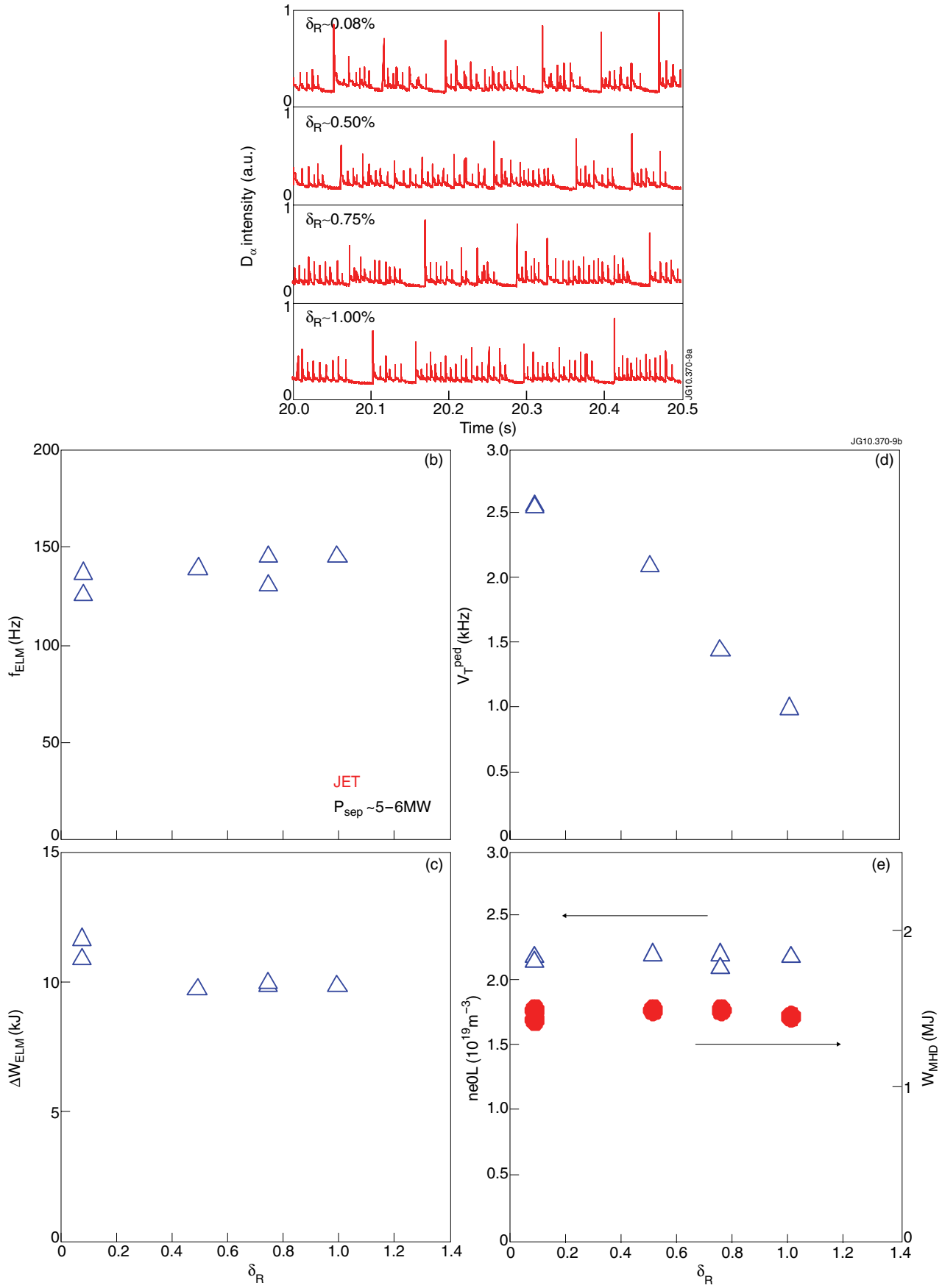

Figure 9: (a) D_α emission intensity at the outer divertor for the variation of TF ripple in JET. Dependence of (b) ELM frequency f_{ELM}, (c) ELM energy loss ΔWELM, (d) edge toroidal rotation frequency V_T^{ped}, (e) line-averaged electron density $\bar{n}_e$, and total stored energy W_{MHD} on the TF ripple amplitude δ_R in JET.

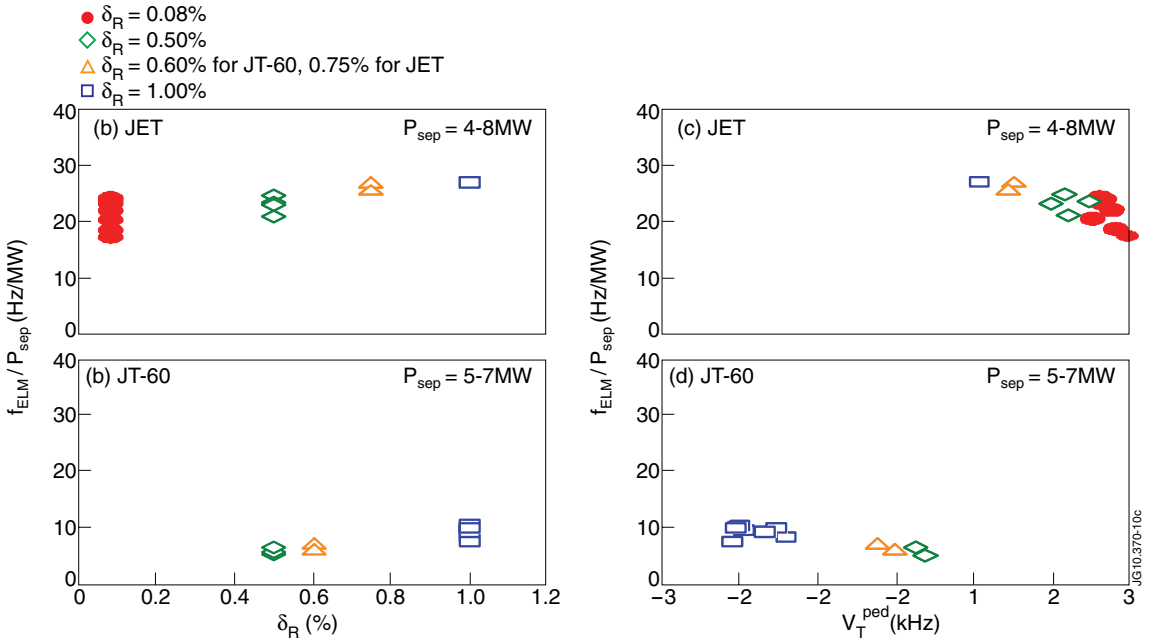

Figure 10: ELM frequency normalized to the power crossing the separatrix f_{ELM}/P_{sep} observed in JET and JT-60U as a function of TF ripple δ_R and V_T^{ped}.

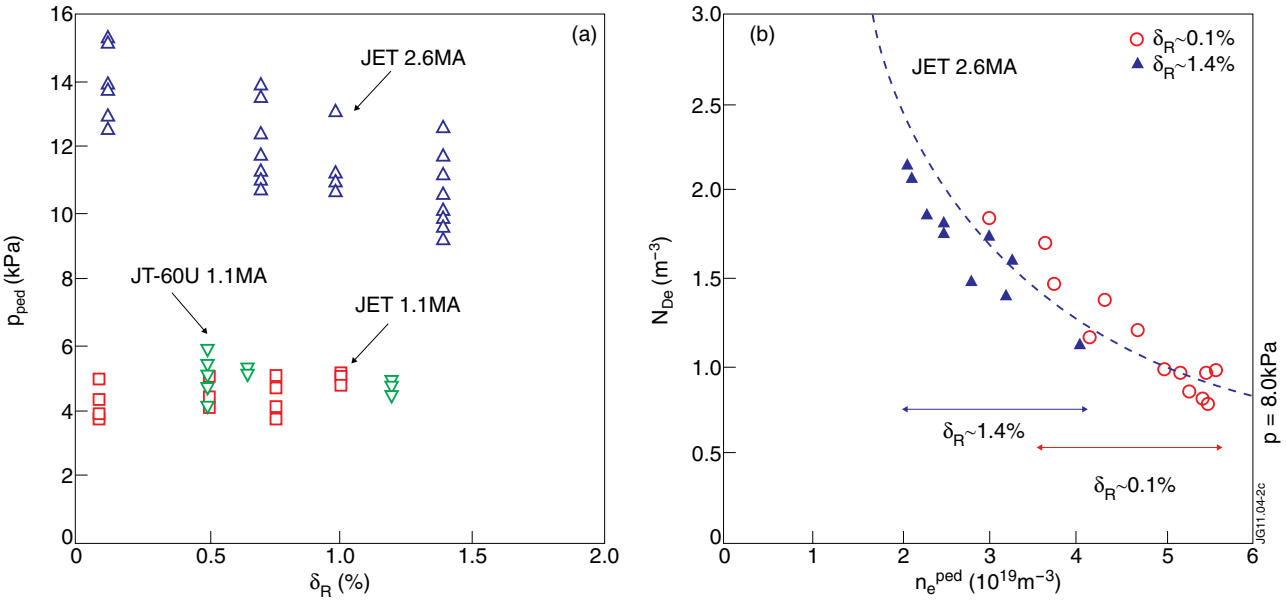

Figure 11: (a) Dependence of pedestal pressure pped on TF ripple δ_R. Squares and inverse triangles indicate the data of the similarity experiment in JET and JT-60U at 1.1MA, respectively. Triangles indicate the data of JET standard configuration at 2.6MA. (b) Pedestal n – T diagram at 2.6MA in JET TF ripple scan for the cases of TF ripple amplitude at the minimum ($\delta_R \sim 0.1\%$) and the maximum (~1.4%). Broken curve indicates a constant electron pressure of 8.0kPa.

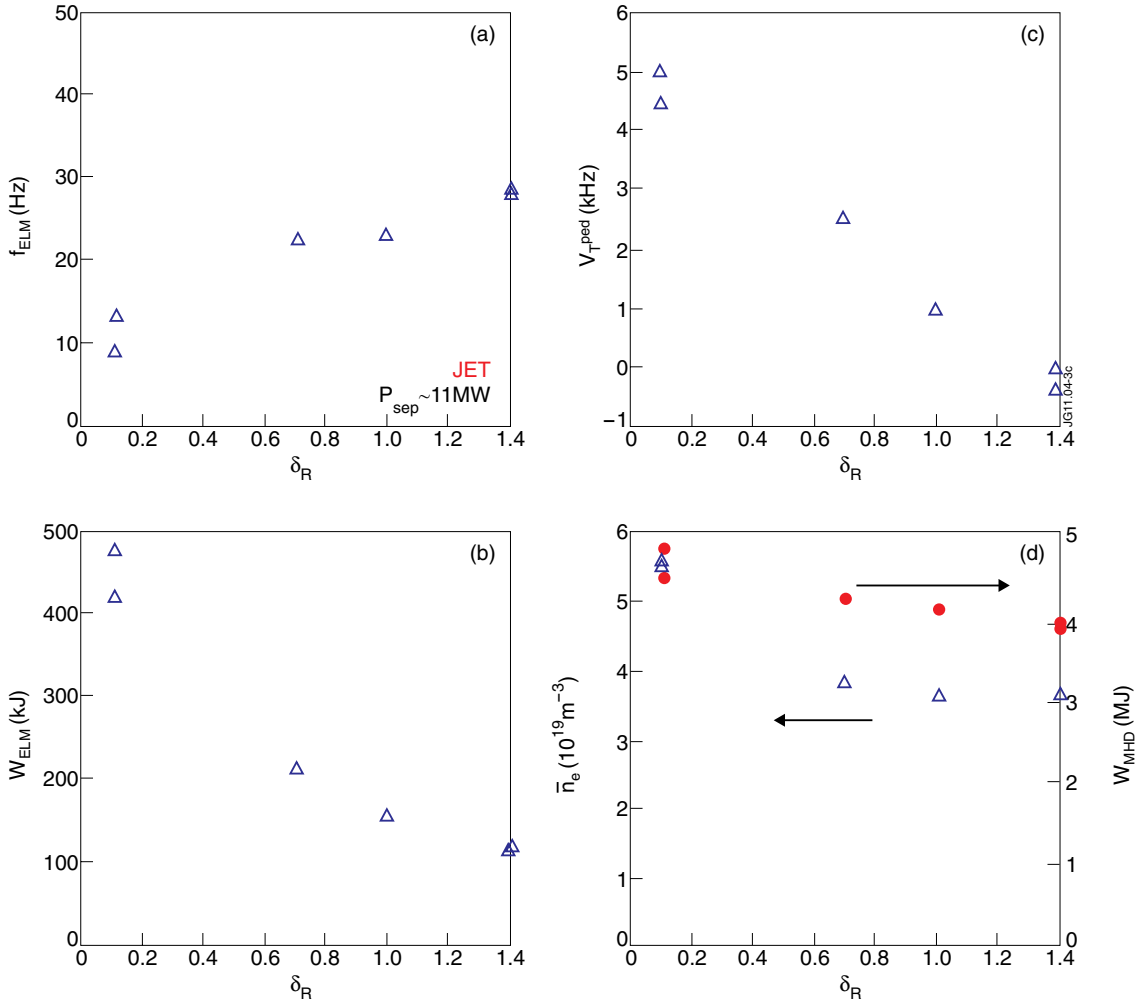

Figure 12. Dependence of (a) ELM frequency fELM, (b) ELM energy loss ΔWELM, (c) pedestal toroidal rotation frequency V pedT , (d) line-averaged electron density ¯ne, and total stored energy on the TF ripple amplitude δR in JET 2.6MA TF ripple scan experiment.